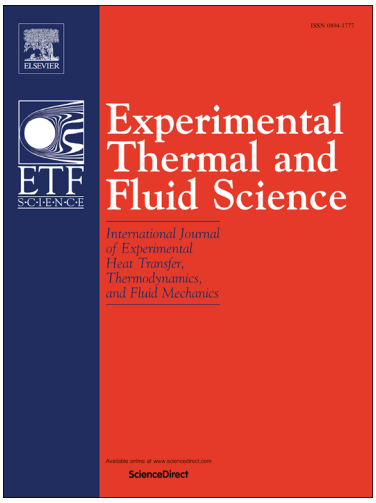


# Influence of Test Model Material on the Accuracy of Transient Heat Transfer Measurements in Impulse Facilities

Qiu Wang, Herbert Olivier, Julius Einhoff, Jinping Li, Wei Zhao

PII: S0894-1777(18)31370-0
DOI: https://doi.org/10.1016/j.expthermflusci.2019.02.013
Reference: ETF 9745

To appear in: *Experimental Thermal and Fluid Science*

Received Date: 10 August 2018
Revised Date: 21 January 2019
Accepted Date: 12 February 2019

Please cite this article as: Q. Wang, H. Olivier, J. Einhoff, J. Li, W. Zhao, Influence of Test Model Material on the Accuracy of Transient Heat Transfer Measurements in Impulse Facilities, *Experimental Thermal and Fluid Science* (2019), doi: https://doi.org/10.1016/j.expthermflusci.2019.02.013

# Influence of Test Model Material on the Accuracy of Transient Heat Transfer Measurements in Impulse Facilities

**Qiu Wang[1,*], Herbert Olivier[2], Julius Einhoff[2], Jinping Li[1], Wei Zhao[1,3]**

[1] *State Key Laboratory of High Temperature Gas Dynamics, Institute of Mechanics, Chinese Academy of Sciences, Beijing, 100190, People's Republic of China*

[2] *Shock Wave Laboratory, RWTH Aachen University, Aachen, 52056, Germany*

[3] *School of Engineering Science, University of Chinese Academy of Sciences, 100049, Beijing, People's Republic of China*

[*] Corresponding author: Qiu Wang, wangqiu@imech.ac.cn

**Abstract:** The development of suitable heat-resistant materials and appropriate thermal structure design for a hypersonic aircraft requires highly precise heat transfer predictions. Unfortunately, existing techniques for measuring the transient heat flux by thermal sensors in impulse facilities are overly complex; any slight deviation from ideal conditions may lead to inaccuracy. In this study, the influence of different model materials leading to lateral heat conduction between model and sensor on the accuracy of heat flux measurements using type-E coaxial thermocouples was investigated. The behavior of the materials results to a deviation from the assumption of one-dimensional heat conduction more or less. The materials examined were stainless steel, aluminum, carbon steel, and polyamide, which are frequently used as model materials in ground tests. The influence of the model materials was estimated by comparing the heat flux derived from the junction temperature with the actual heat flux loading. Particular attention was paid to aluminum, which is extensively used as wind tunnel model material. An engineering-based approach is also presented to conduct high accuracy measurements. The results show that the difference in the thermal properties between the sensor and the model materials creates complicated lateral heat conduction between them; stainless steel 304 is suggest as the use of model material whenever high-accuracy heat transfer measurements are desired due to its similarity of the thermal properties to type-E sensors. The use of polyamide PA6 material resulted in a larger heat flux due to its smaller thermal effusivity and the aluminum and carbon steel led to lower heat fluxes due to their larger thermal effusivity. The deviation of either material increases over testing time.

**Keywords:** Heat transfer measurement; Lateral heat conduction; Shock tunnel; Thermocouple; Hypersonic

## I. Introduction

The accurate prediction of aerodynamic heating is important for the design and development of hypersonic flight vehicles, and its prediction often remains difficult by modern computational fluid dynamics (CFD). Experimental measurements still play an indispensable role in addressing this problem. Due to the high costs and complexity of flight tests, most aerodynamic heating experiments are performed in ground impulse facilities, like shock tunnels and shock tubes, for which the available test time is usually in the order of a few milliseconds. However, experimental data of high accuracy is challenging to obtain. Nevertheless, this data is also important for the calibration and validation of CFD codes, especially for thermal and chemical nonequilibrium conditions. Therefore, there is an urgent need for improving the measuring accuracy and reducing the uncertainties associated with the predictions of aerothermal test data.

Transient heat transfer measurements in impulse test facilities are performed by capturing the transient temperature rise of the sensor, flush-mounted in the wall of the test model. The time-resolved data is then processed to calculate the heat flux by applying a physical heat conduction model with few, mostly simplified assumptions. Generally, the techniques can be divided into two categories: one based on the use of heat flux sensors, such as resistance thermometers, thermocouples, and calorimeters, and the other based on non-intrusive techniques such as temperature sensitive paint and thermography. However, each technique has its own advantages and challenges. Because of the technologically immature nature of non-intrusive techniques, heat flux sensors that are typically cylindrical in shape, are still primarily used for heat transfer measurements, especially in high enthalpy facilities [1]. There is, of course, a tremendous amount of literature pertaining to this subject and ranging from experimental techniques to analytical and computational analyses [2-4]. Any improvements in the heat transfer measurements necessitate an in-depth investigation of the technique, including gauge installation, gauge calibration and sensitivity tests, data reduction procedures, the analysis of gauge size effects, and uncertainties. For example, Sanderson [5], Marineau [6], the Shock Wave Laboratory [7] and Li [8] conducted intensive studies on the design, modeling, and calibration of coaxial thermocouples and great progress was made. The coaxial thermocouples have been demonstrated to be accurate and reliable for short-duration transient temperature measurements and they have especially performed well in high enthalpy shock tunnels with harsh hypersonic freestream flow environment. Often the flow contains small particles of metallic and nonmetallic materials which pose problems to the mechanical integraty of other sensors but not of the coaxial thermocouples. They are also widely used in many other applications, such as gun barrel studies [9], internal combustion engine heat transfer measurements [10] and boiling research [11]. In another study, Wang [12] examined the influence of the sensor installation on the accuracy of heat transfer measurements; protruding installation led to a larger heat flux and recessed to lower ones compared to the reference heat flux loading. There have also been made valuable suggestions for sensor installation to improve the accuracy.

Although much progress has been made in improving the accuracy of heat transfer measurements in recent decades, often there is still a difference of ±10 % between experimental and theoretical results e.g. for a sharp cone standard model [13]; the difference might be even larger at certain local regions of more complex model shapes [14]. It remains necessary to extensively investigate the factors and rules influencing the heat transfer measurements before further progress can be made.

For highly transient heat transfer measurements, the heat flux is mostly derived from the monitored surface temperature signal employing the essential assumption of one-dimensional, semi-infinite heat conduction within the sensor. Any deviation from this assumption leads to inaccuracy. In reality, however, it is hard to meet this assumption. For example, coaxial thermocouples consist of at least three different materials with different thermal properties, including two thermocouple materials and one insulation material and the thermal environment is inevitably non-homogeneous [15]. Li [8] numerically investigated the heat conduction within a type-E coaxial thermocouple. He pointed out that the actual heat conduction process near the junction deviates strongly from that described by the commonly used one-dimensional heat conduction theory due to the heat blocking effect of the insulation layer. His study provided reference information for the fabrication of surface junction thermocouples. However, it is focused only on the heat conduction inside the thermocouples.

Since the majority of type-E coaxial thermocouples consist of a chromel annulus on the outside, the sensor ideally should be installed into a model with chromel material in order to best match the thermal properties. However, this approach is structurally and financially prohibitive. Stainless steel, aluminum, and carbon steel are frequently used as model materials in ground tests and their thermal properties differ from those of typical sensors or thermocouples. Thus, a lateral heat transfer between the model and the sensor inextricably exists, substantially affecting the accuracy of the heat transfer measurements. In particular, aluminum alloy is a favorite choice for test models due to its relatively low density and excellent mechanical machining properties. It is a preferred model material for large impulse facilities, such as the JF12 shock tunnel, where the nozzle exit diameter amounts to 2.5 m. A typical test model has a length of 3–5 m and a weight of several hundred kilograms [16, 17]. Aluminum significantly reduces the model weight; however, the significant difference in its thermal properties to those of the sensor leads to problems for the heat transfer measurements. Moreover, the effective test time of large impulse facilities are extended as the technology has improved. For example, the test time of the JF12 shock tunnel amounts to 100 ms, which is approximately an order of magnitude longer than that of conventional shock tunnels. This further complicates the unsteady heat conduction between the model and the sensor, affects the accuracy of measurements, and challenges the one-dimensional heat conduction assumption. For these reasons, heat transfer measurements at these conditions still need extensive research.

In the present study, type-E coaxial thermocouples have been used, which were fabricated by the Shock Wave Laboratory and which have been widely used. The influence of different test model materials on the accuracy of heat transfer measurements is examined first by a series of experiments. Furthermore, the temperature distribution and heat transfer within the sensor and model are examined by solving the two-dimensional heat conduction equations numerically. Corresponding fundamentals and mechanisms are discussed in detail, which provide information on the inevitable measurement uncertainty caused by lateral heat conduction between sensor and model. Particular attention was focused on aluminum as test model material because of its extensive use. Other factors that may influence the measurement accuracy, such as the sensor diameter or a possible placement of a stainless steel tube between the sensor and the model material, are also discussed. In all, this investigation provides guidance for a suitable design of test models regarding heat flux measurements in impulse facilities and shows how to improve the measuring accuracy.

## II. Experimental Techniques

### A. Experimental setup

Heat flux measurements in impulse facilities are extremely sensitive to many physical factors, like the free-stream flow uniformity, gas purity and others. In addition, the measuring uncertainty caused by these factors makes it difficult to analyze the influence of different model materials on the measuring accuracy. Therefore, heat flux measurements were performed with a radiative heat flux source at the Shock Wave Laboratory (SWL) of RWTH Aachen University, Germany. A relatively simple model configuration was selected to reduce the uncertainties coming from a complex model geometry. For simplicity, the coaxial thermocouples were installed into a cylinder with 28 mm diameter and a thickness of 10 mm (see Fig. 1). Three different materials, stainless steel (304), aluminum (7075), and polyamide (PA6), were tested. The first two materials are frequently used for wind tunnel models in impulse facilities. To fully elucidate

the relevant physical mechanisms, polyamide was also tested here for its relatively different thermo-physical parameters from the other two, although it is not widely used as wind tunnel model material.

A type-E coaxial thermocouple built by the SWL was installed at the center of the cylindrical body. The diameter of the thermocouple is 1.9 mm and its thermal calibration factor is $\sqrt{\rho ck}$ = 8600 W·s$^{0.5}$/(m$^2$·K). The contact method is used to calibrate the thermocouple. The uncertainty of the calibrated $\sqrt{\rho ck}$ value is within 6 %. Details about the calibration can be found on the homepage of the Shock Wave Laboratory [7]. The calibration of the temperature sensitivity shows that it perfectly agrees with published values e.g. in the NIST tables [18]. The thermocouple junction was formed by abrading the top surface of the thermocouple with sandpaper. It has to be emphasized that some measures were taken to ensure consistency of the different test cases. First, the same sensor was used for all the experiments; the influence comes to uncertainty of $\sqrt{\rho ck}$ to our conclusions can be eliminated. After the sensor was installed, the model surface was painted black in a repeatable way with Super-Therm heat-resistant paint, which eliminates the difference in the emissivity of the different model materials. Thus, the model surface could be treated as thermally black and all the energy from the calibration system was absorbed by the model and the sensor surface. Although the thickness of the paint has influence on the response time of the thermocouples, the test time in our experiments is long enough to neglect this influence. Thus, the heat conduction within the paint was not considered in this paper.

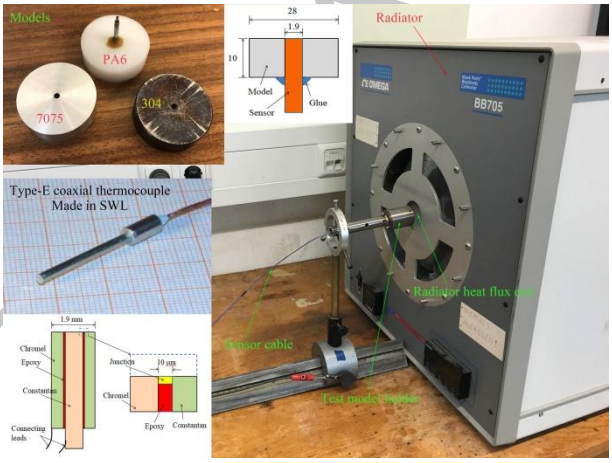


**Fig. 1 Radiative heat flux source and test bodies; units in *mm*.**

The same voltage amplifier was used to amplify the output of the type-E thermocouple at a gain factor of 1000. The signals from the sensors were acquired by a signal conditioner and processed on a PC-based data acquisition system at a sampling rate of 100 Hz. The same low-pass filter was used for all measurements to eliminate high-frequency spurious components.

From the measured surface temperature *T*, the heat flux $\dot{q}$ is calculated according to Schultz and Jones [19] by a solution of the transient one-dimensional heat conduction equation, Eq. (1),

$$\dot{q}(t_n) = 2\sqrt{\frac{\rho ck}{\pi}} \sum_{i=1}^{n} \frac{T(t_i) - T(t_{i-1})}{\sqrt{t_n - t_i} + \sqrt{t_n - t_{i-1}}} \tag{1}$$

where $\rho$, $c$ and $k$ are the density, heat capacity, and heat conductivity of the sensor material; $T$ and $t$ are the temperature and time, respectively. This equation is valid at least for the beginning of the relatively long measuring time shown in this paper.

### B. Experimental Results

First, the repeatability of the experiments and the measurements has been checked. Figure 2 shows the obtained heat flux histories for three measurements for the same nominal test condition. For the three tests, the standard deviation of the heat flux is about 1.7 %. The averaged heat flux amounts to 7200 W/m$^2$.

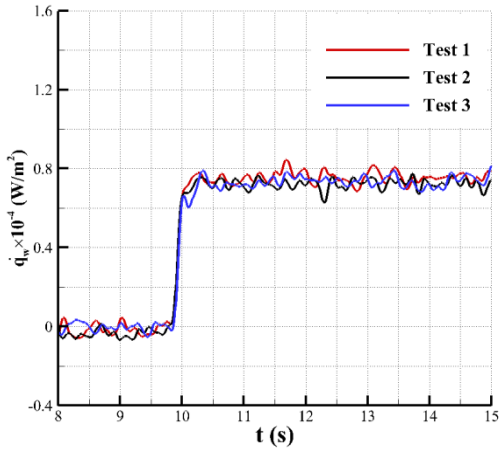


**Fig. 2 Heat flux of repeated experiments for stainless steel model material.**

Typical temperature signals and corresponding heat fluxes for different model materials derived from Eq. (1) are shown in Fig. 3. Since the wall thickness of the test models is only 10 mm, the results of the first several seconds are showed here. Although the test time here is much longer than the effective test time in an impulse facility, there is a clear difference between the three materials from the very beginning. Polyamide (PA6) results in a higher temperature rise and heat flux than the stainless steel body (304). The aluminum cylinder (7075) yields a lower heat flux than the stainless steel one.

For a constant heat flux into a semi-infinite body, the surface temperature change can be obtained by a solution of the transient one-dimensional heat conduction equation, shown in Eq. (2):

$$\Delta T = \frac{2\dot{q}}{\sqrt{\pi}}\sqrt{\frac{t}{\rho c k}} \tag{2}$$

The relationship $\Delta T \propto \sqrt{t}$ shows that the measured signal should follow a parabolic trend since the radiative heat flux $\dot{q}$ is constant and the value of $\sqrt{\rho c k}$ can also be considered constant due to the small temperature increase during the measurement. This behavior is well represented by the temperature signal for stainless steel in Fig. 2. The dissimilarity in the trends of polyamide (PA6) and aluminum (7075) with stainless steel 304 also suggests that the heat conduction between sensor and model is different for the three model materials.

Table 1 shows that the $\sqrt{\rho c k}$ value of 304 is close to that of chromel/constantan, which results in similar surface temperatures for the sensor and the model surface. Thus, the heat exchange between 304 and the sensor is small. The

lower $\sqrt{\rho ck}$ value of PA6 results in a higher surface temperature than the sensor, while 7075 has a smaller one. The surface temperature difference between model and sensor causes lateral heat transfer close to the surface, which does not meet the one-dimensional assumption. Namely, polyamide will transmit energy to the sensor resulting in a higher temperature signal and therewith heat flux, while aluminum absorbs energy from the sensor resulting in a lower heat flux. This is the reason for the temperature and heat flux differences observed in Fig. 3. Even worse, the heat fluxes for PA6 and 7075 are unsteady and change markedly over time as shown in Fig. 3. This makes it difficult to use a correction factor for the different materials.

**Table 1 Thermo-physical parameters of the materials [20]**

| Materials | Constantan | Chromel | Stainless steel, 304 | Aluminum 7075 | Carbon steel (0.5% C) | Polyamide PA6 |
|---|---|---|---|---|---|---|
| $\rho$, kg/m$^3$ | 8920 | 8730 | 7930 | 2800 | 7833 | 1140 |
| $c$, J/(kg·K) | 393.1 | 447.5 | 500 | 960 | 465 | 1600 |
| $k$, W/(m·K) | 21.17 | 19.25 | 17 | 130 | 54 | 0.37 |
| $(\rho ck)^{0.5}$, W·s$^{0.5}$/(m$^2$·K) | 8616 | 8672 | 8210 | 18693 | 14025 | 822 |

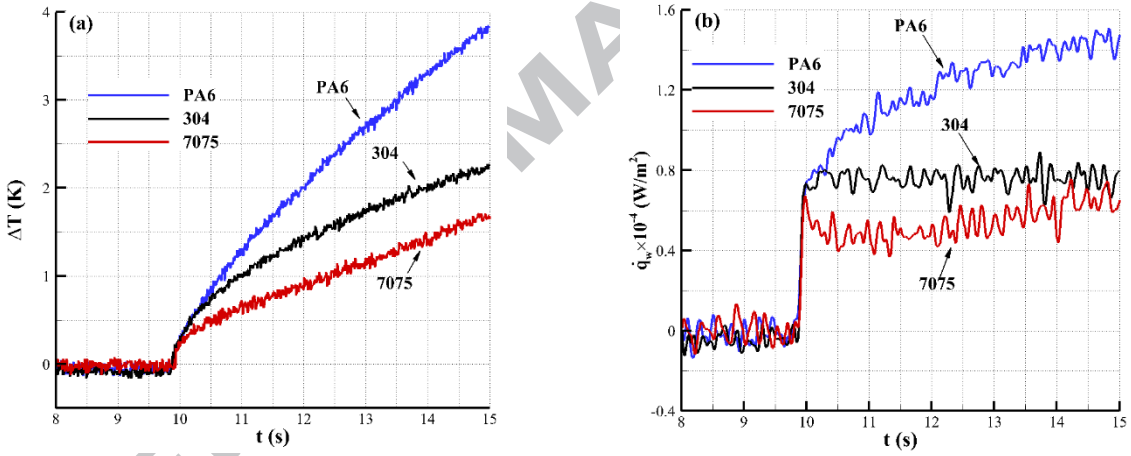


**Fig. 3 Experimental results for different model materials. (a) surface temperature, (b) heat flux.**

For obtaining a better understanding of the lateral heat transfer between sensor and model, a thermal insulation layer has been placed between the sensor and the aluminum body. The setup with heat-resistant paint or a gap as insulation is shown in Fig. 4. The paint insulation has a thickness of about 0.02 mm where the outer side of the thermocouple is coated with Super-Therm heat-resistant paint. The gap, which uses air as insulation, has a thickness of about 0.2 mm. Because the heat-resistant paint and the air gap have a very small heat conductivity, they significantly reduce the heat transfer between sensor and model. The corresponding results are shown in Fig. 4 and indicate that the gap results in the same heat flux as the 304 stainless steel material, which is regarded as reference heat flux. The paint insulation results in a smaller heat flux than the 304 material but a higher one than the 7075 material. This result is expected, since the higher the thermal resistance of the insulation layer, the less heat is transferred between sensor and model. The air gap blocks most of the lateral heat flux whereas the paint insulation only blocks part of it.

From these results it can be concluded that test model materials with obvious different thermal properties as the sensor ones significantly affect the heat transfer measuring accuracy. Unfortunately, these experiments cannot demonstrate the heat energy exchange between sensor and model in detail and the experimental setup did not allow a time resolution in the millisecond range. However, they clearly show at least qualitatively the influence of lateral heat conduction. Thus, further investigations using numerical simulations were carried out.

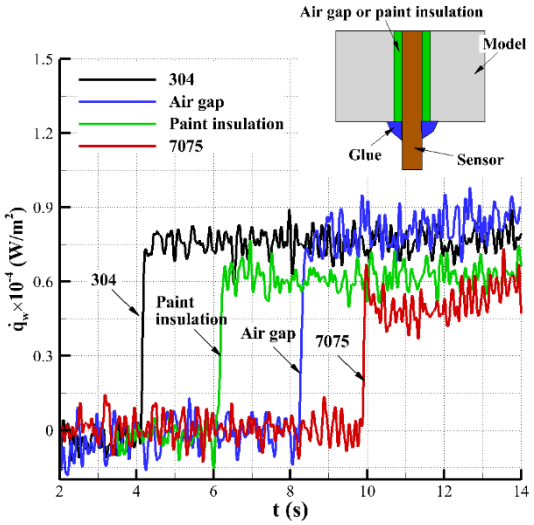


**Fig. 4 Heat flux histories for a paint and air gap insulation.**

## III. Numerical Simulations

### A. Simulation Methodology

To provide a valuable complement to the experimental results and to better understand the heat exchange between sensor and model, especially for the first several milliseconds, numerical simulations have been conducted because of its easier operation and detailed information. The governing equation employed is the axisymmetric unsteady heat conduction equation:

$$\frac{\partial T}{\partial t} = \frac{k_i}{\rho_i c_i}\left(\frac{\partial^2 T}{\partial x^2} + \frac{\partial^2 T}{\partial r^2} + \frac{1}{r}\frac{\partial T}{\partial r}\right) \quad (i = 1, 2) \tag{3}$$

where $x$ and $r$ are the axial and radial coordinates of the physical space; $\rho$, $c$ and $k$ are the density, heat capacity and heat conductivity of the material, $T$ and $t$ are the temperature and time, respectively. The subscripts 1 and 2 denote the sensor and the model, respectively. Eq. (3) is solved using a finite difference method for the spatial discretization and a fourth order Runge-Kutta method for time integration [21].

As in the experiments, the simulated model wall has a thickness of 10 mm and a cylindrical shape with 28 mm diameter. Considering the axial symmetry of the computational model, half of the geometry has been considered as shown in Fig. 5. The radius of the sensor is indicated by $r_s$ and given by 0.95 mm. Structured grids are applied; the zones near the surface and the sensor/model interface are incorporated with clustered points to provide good spatial resolution. A grid convergence study was conducted for three different grid resolutions (401×401, 601×601 and 801×801 grid points) and aluminum as model material. There was a negligible difference of the junction heat flux normalized by the loading

heat flux for all grids as shown in Fig. 6. Finally, the grid with 601×601 grid points was employed for the present study. It is worth to mention that Fig. 6 shows the same peak heat flux behavior at the beginning of the thermal loading as the experiment shown in Fig. 3.

The initial temperature of the sensor is set to $T_\infty$ = 295 K for the calculation. Since the heat transfer rate from the radiator to the sensor is constant in the experiments, for the simulations a constant heat flux $\dot{q}$ is also uniformly applied on the top surface, i.e., $\left(\frac{\partial T}{\partial x}\right)_{x=0} = \frac{\dot{q}_w}{k_i}$ $(i = 1, 2), t > 0$. The other boundary conditions are shown in Fig. 5. An adiabatic boundary condition is applied to the right and lower boundaries including the model and sensor, and a symmetric boundary condition for the left. In addition, temperature and heat flux satisfy the continuity condition at the interface between the two different materials.

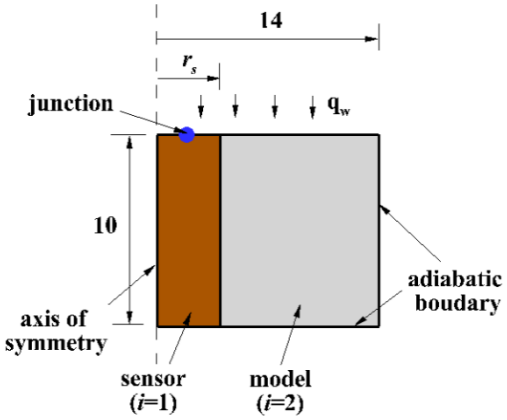


**Fig. 5 Schematic drawing of the simulated model (not to scale, units in *mm*).**

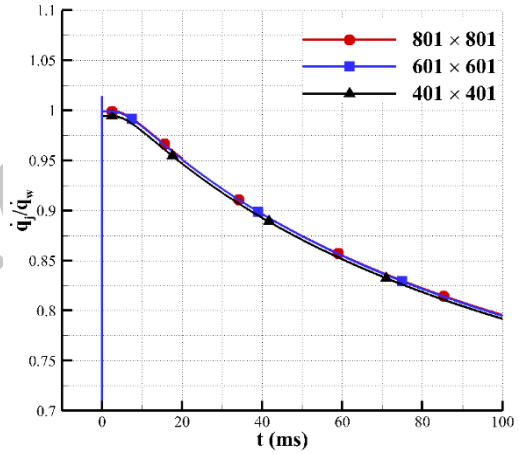


**Fig. 6 Junction heat flux for three grid resolutions.**

To provide theoretical guidance for the thermomechanical design of models and to obtain the best solution for high accuracy heat transfer measurements, four materials have been considered: stainless steel (304), carbon steel (0.5 % C), aluminum (7075), and polyamide (PA6), where the first three are commonly used. Aluminum is of special interest as mentioned above for large wind tunnel models. The physical material parameters used in the calculations are shown in Table 1. For the considered short times, i.e. small temperature changes, these parameters are assumed to be constant with temperature. Considering the very close properties of chromel and constantan for a type-E coaxial thermocouple and for simplification in computation, the parameters of constantan are chosen to represent the sensor. The sensor junction in the experiments and numerical simulations is located at half of the sensor radius, as shown in Fig. 5. Since the thickness of the insulation layer between chromel and constantan is approximately 10 μm, it is acceptable to fix the junction position at one grid point at this position for which the heat flux is determined.

### B. Comparison with Experimental Results

As in the experiments, the heat flux $\dot{q}_w$ = 0.72×10$^4$ W/m$^2$ is used as the loading heat flux on the top surface in the following simulations. A comparison between experimental and numerical data for the junction temperature and the heat flux derived from Eq. (1) is shown in Fig. 7 for aluminum as model material. The results show a good agreement between experimental and numerical results for both of them. It needs to be noted that there would be heat diffusion from the sensor to the air on the bottom side in our experiments. However, since the air has very small heat conductivity, the heat diffusion is negligible for the top surface heat transfer calculation. This can be also verified in Fig. 4 that the air gap blocks the lateral heat flux and results in the same heat flux as the 304 stainless steel material. In case of the air gap insulation the thermocouple has no thermal contact to the model material. But in case of the stainless steel model it has. Since in both cases the same heat flux level is achieved, the different type of sensor installation, especially at the bottom wall, is of no influence. As mentioned above, due to the low heat conductivity of air, the heat transfer from the model into the air is very small. Therefore, the adiabatic boundary condition is applied on the bottom side for all cases.

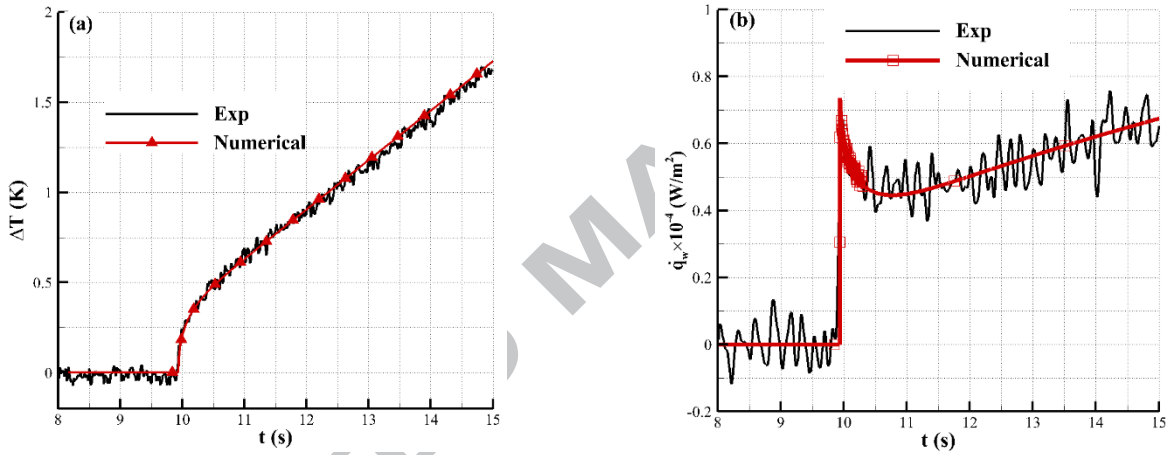


**Fig. 7 Comparison of experimental and numerical results. (a) surface temperature, (b) heat flux.**

Figure 8 shows the simulated temperature distribution inside and on the top surface of the sensor for aluminum as model material at the moment of $t$ = 70 ms. As expected, a more complicated heat conduction process inside the model takes place. First, the temperature along the top surface of the computing model is not constant and the larger $\rho ck$ value of aluminum results in a lower surface temperature than for the sensor. However, the heat transfers faster within the aluminum in the $x$-direction than along the sensor, which results in higher temperature than for the sensor at the bottom regions, as shown exemplarily for $x$ = 1.28 mm in Fig. 8(b). Thus, the thermal environment of the sensor is complex; dissipating energy laterally to the model at the surface region, but absorbing heat from its bottom neighbor, as indicated by the arrows in Fig. 8(a); this complexity certainly affects the temporal changes in the junction temperature that is of interest for the heat flux measurements. These findings disagree with the assumption of one-dimensional heat transfer due to the different thermo-physical parameters of aluminum 7075 and the sensor material. Therefore, Eq. (1) derived by a solution of the transient one-dimensional heat conduction equation is inappropriate here and leads to a significant error in the experiments as shown for the initial measuring phase for aluminum in Fig. 3.

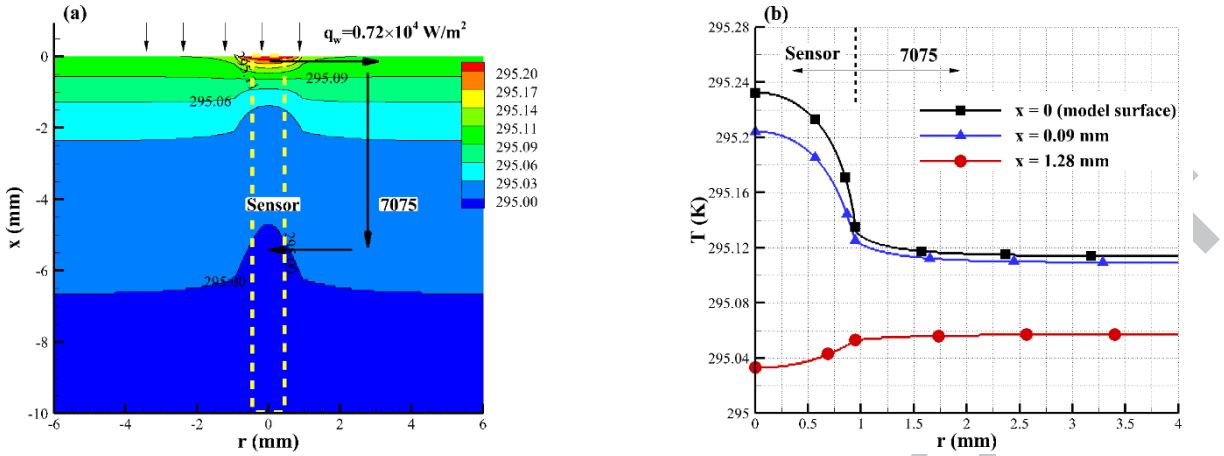


**Fig. 8 Temperature distribution for aluminum as model material at 70 ms. (a) temperature field inside the model, (b) temperature distribution at x = 0 (model surface), x = 0.09 mm and x = 1.28 mm.**

Additionally, since the thickness of the model is 10 mm, it takes about 200 ms for the heat energy to transfer from the aluminum surface to the bottom due to its high heat conductivity [19]. However, this time interval is much longer for the other materials with smaller heat conductivity shown in Table 1. The average temperature increase after about 200 ms can be estimated as $\frac{\Delta T}{\Delta t} = \frac{\dot{q}_w}{\rho c l}$, where $l$ is the model wall thickness. This shows that the temporal temperature gradient is higher for aluminum than for the sensor due to its smaller $\rho c$ value. The energy transfer rate from the sensor to the model subsequently decreases over time. This is the reason for the heat flux increase for the aluminum material in Fig. 2 after about 12 seconds. Nevertheless, our concern is the heat transfer in impulse facilities, especially in shock tunnels, where the effective test time is usually no longer than 100 ms. Therefore, in the following the discussion is mainly focused on this time period.

### C. Numerical study of the influence of the model material

In this chapter the time-dependent influence of the model material is studied by numerical simulations. For this, the heat flux ratio $\dot{q}_j/\dot{q}_w$ is considered, where the heat flux $\dot{q}_w$ represents the heat flux loading on the sensor and model surface and $\dot{q}_j$ is derived from the junction temperature as in the experiments. It is noteworthy that although the magnitude of $\dot{q}_w$ affects the temperature increase (as seen from Eq. (2)), or, the temperature difference between sensor and model increases with a higher $\dot{q}_w$. However, it has no influence on the non-dimensional value of $\dot{q}_j/\dot{q}_w$ in the present study, as shown in Fig. 9. Thus, a higher heat flux loading than 0.72×10$^6$ W/m$^2$ is used to obtain a more significant surface temperature increase in the following calculations. This finding also indicates that the results and conclusions are independent for the transient heat transfer measurement from the absolute heat flux loading. Also to note is that the heat flux loading $\dot{q}_w$ is constant with time, which is a reasonable approximation for heat transfer measurements during the effective test time of impulse facilities.

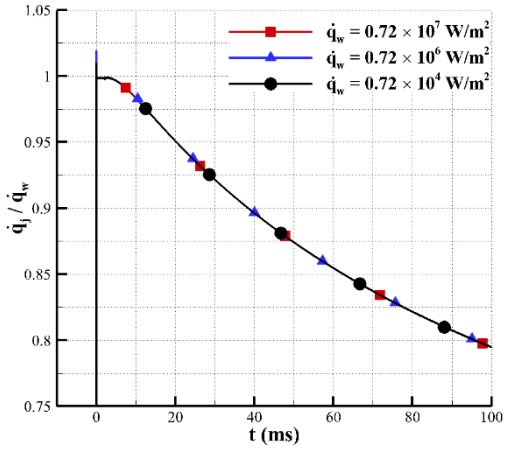


**Fig. 9 Heat flux ratio $\dot{q}_j/\dot{q}_w$ versus time for different heat flux loading; model material aluminum.**

Figure 10 shows the heat flux ratio for the sensor (diameter of 1.9 mm) installed in different model materials. During the first period of time when $\dot{q}_j/\dot{q}_w$ approaches 1 for all materials, the model material has negligible effect on the junction temperature or heat flux. For the considered sensor diameter this period lasts for about 5 ms. If the test time of an impulse facility is within this period, there is no need to consider the influence of the model material or lateral heat conduction while conducting heat flux measurements. After this period, the different materials result in different heat fluxes. The PA6 yields a higher heat flux than the loading heat flux, $\dot{q}_j/\dot{q}_w$ increases over time with a deviation of about 11.2 % after 100 ms. In contrary, aluminum and carbon steel result in lower heat fluxes with a deviation of about 20.5 % and 13 % after 100 ms, respectively. Fig. 11 shows the temperature distribution on the top surface of the model at $t$ = 100 ms. Polyamide results in a higher surface temperature than the sensor, aluminum and carbon steel to a lower one, which is in agreement with the discussion in section 2.2. Thus, polyamide transfers energy to the sensor at the surface leading to higher junction temperature and therewith larger heat flux, whereas aluminum and carbon steel absorb heat from the sensor leading to lower heat fluxes. This deviates from the one-dimensional heat conduction assumption as expected and therefore leads to an inaccuracy of the deduced heat flux.

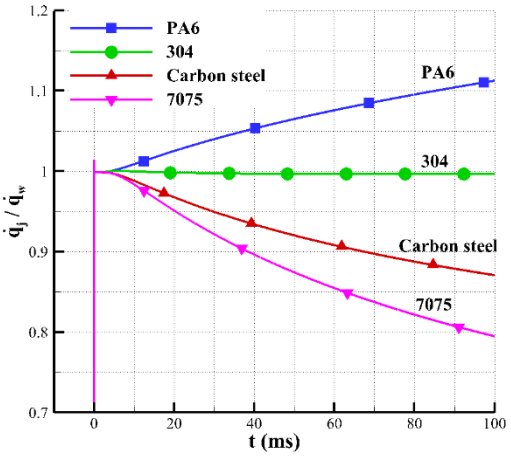


**Fig. 10 Heat flux ratio $\dot{q}_j/\dot{q}_w$ versus time for different model materials.**

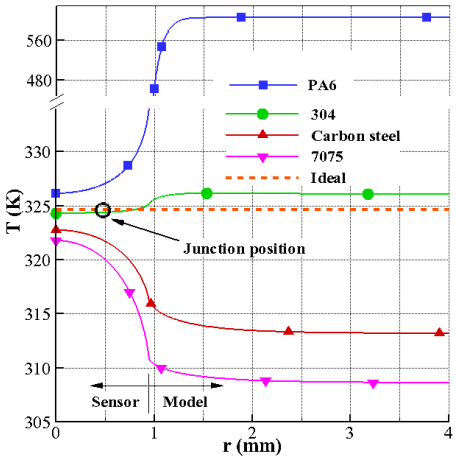


**Fig. 11 Surface temperature distribution at $t$ = 100 ms.**

As expected, the ratio $\dot{q}_j/\dot{q}_w$ for stainless steel is fairly close to one, which means the influence of this model material on the measuring accuracy is very small (less than 1 %). In addition, it indicates that the approach of using the heat flux for the stainless steel model as the heat flux loading for the numerical simulations is reasonable. Thus, it is recommended to use stainless steel as model material whenever high-accuracy heat transfer measurements are desired.

### D. Engineering-based approach

As described above, the use of aluminum as model material is of certain advantage but would lead to problems for testing times longer than 5 ms or small sensor diameters. The air gap insulation shown in Fig. 4 is able to solve this problem for the considered case of a radiative heat flux source where there is no gas flow. However, for a wind tunnel model the gap would affect the local surface of the model, it substantially would disturb the gas flow passing the sensors leading to experimental inaccuracy, and with ongoing time it would be obstructed by small particles, which are always present in the flow. To overcome these problems, it is recommended to place the thermocouple into a stainless steel tube, which in fact increases the distance between the junction and the sensor's cylindrical outer wall. The influence of this combination on the measuring accuracy has been studied by numerical simulation.

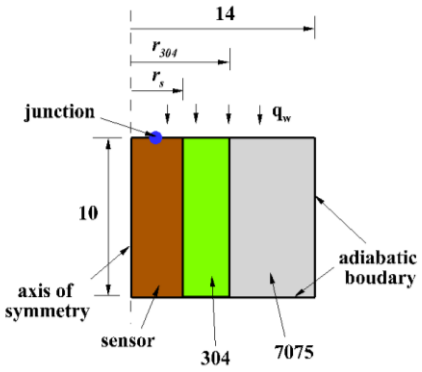


**Fig. 12 Schematic diagram of the sensor with stainless steel tube installed into an aluminum model (not to scale, units in *mm*).**

In Fig. 12, $r_{304}$ is the radius of the stainless steel tube and $r_s$ = 0.95 mm is the radius of the sensor. $r_{304}$ is varied to 2 mm, 3 mm, and 4 mm, respectively. The heat flux ratio $\dot{q}_j/\dot{q}_w$ and surface temperature distributions are shown in Fig. 13 and Fig. 14. It is apparent that the stainless steel tube effectively solves the problem of severe lateral heat conduction in aluminum models. Within 40 ms, the ratio $\dot{q}_j/\dot{q}_w$ and therewith the heat flux is the same for all three tube radii. After this time, the heat flux for the 2 mm tube decreases over time, whereas the other two remain constant. However, even the tube with 2 mm radius results in a measuring deviation less than 2 % after 100 ms. The deviation is less than 1 % for the 3 mm and 4 mm cases. Thus, a stainless steel tube with an outer radius of 3 mm or larger is fully sufficient for 100 ms test time allowing to combine the advantages of stainless steel for heat transfer measurements and of aluminum as model material.

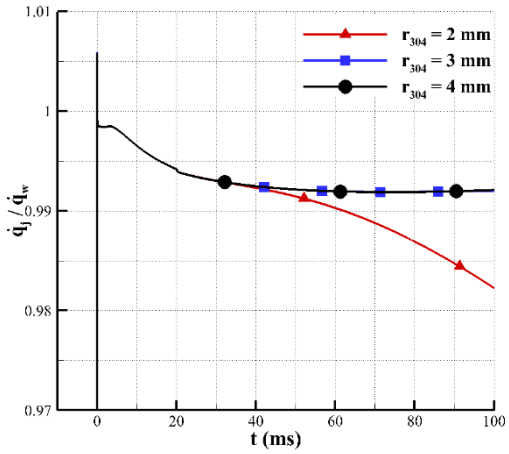


**Fig. 13 Heat flux ratio $\dot{q}_j/\dot{q}_w$ versus time for three different tube radii.**

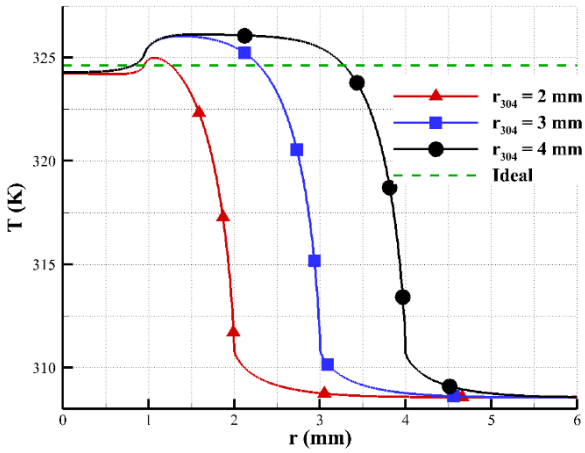


**Fig. 14 Surface temperature distribution at *t* = 100 ms.**

Since the $\sqrt{\rho ck}$ value of 304 is quite close to that of the sensor as shown in Table 1, the stainless steel tube has the similar effect as enlarging the diameter of thermocouple. Ultimately, the larger the sensor, the larger the distance is between the sensor junction and the test model, and the smaller the impact is of the lateral heat conduction on the junction temperature. It can also be concluded that a coaxial thermocouple with an inner constantan wire of small diameter is better suited to locate the junction further away from the surrounding test model material. These observations suggest that the model material, the test time of the facility and the sensor diameter should be taken into consideration whenever high-accuracy heat transfer measurements are desired.

## IV. Conclusion

This study shows by experiments and numerical simulations the influence of the model material on the accuracy of transient heat transfer measurements performed with coaxial surface thermocouples. The different thermal properties of the sensor and the model material lead to lateral heat conduction between both. Consequently, the thermal behavior of the sensor deviates from the commonly used one-dimensional heat conduction model. Within a certain period of time, which is mainly determined by the sensor diameter, this lateral heat conduction has negligible effect on the measuring accuracy. Beyond this period, it leads to an inaccuracy except for stainless steel as model material, which has thermal properties similar to those of the considered type-E coaxial thermocouple. There is no doubt that stainless steel is the optimal choice as model material. Polyamide results in higher heat fluxes than the real heat flux. The deviation increases over time reaching about 11.2 % after 100 ms. In contrast, aluminum and carbon steel lead to lower heat fluxes with a deviation of about 20.5 % and 13 %, respectively. The results also show, the smaller the sensor diameter, the more severe is the deviation. For aluminum as wind tunnel model material, which has the advantages of relatively low weight and excellent machining properties, a stainless steel tube with an outer radius of 3 mm or larger is recommended to cover the coaxial thermocouple. In this case highly accurate heat flux measurements are possible even for long testing times of about 100 ms. In short, the lateral heat

conduction between the sensor and model has to be taken into consideration to ensure reliable heat transfer measurements.

## Acknowledgments

This work was supported by the China Scholarship Council and the National Natural Science Foundation of China (Grant Nos. 11402275 and 11472280), which is gratefully acknowledged by the authors. Most of the presented work has been performed during a research stay of the first author at the Shock Wave Laboratory of RWTH Aachen University. The experimental support of the laboratory and fruitful scientific discussions with the members of the Shock Wave Laboratory are also gratefully acknowledged.

## References

[1] Wu, S., Shu, Y. H., Li, J. P., and Yu, H.R., "An Integral Heat Flux Sensor with High Spatial and Temporal Resolutions," *Chinese Science Bulletin*, Vol. 59, No. 27, 2014, pp. 3484-3489.
doi: 10.1007/s11434-014-0464-6

[2] Zeng, L., Gui, Y. W., Wang, A. L., Qin, F., and Zhang, H. Y., "Study on Error Mechanism and Uncertainty Assessment of Heat Flux Measurement in Shock Tunnel," *Journal of Experiments in Fluid Mechanics*, Vol. 29, No. 5, 2015, pp. 15-25.
doi: 10.11729/syltlx20140135

[3] Coblish, J. J., Coulter, S. C., and Norris, J. D., "Aerothermal Measurement Improvements using Coaxial Thermocouples at AEDC Hypervelocity Wind Tunnel No. 9," *45th AIAA Aerospace Sciences Meeting and Exhibit Reno*, Nevada, AIAA Paper 2007-1467, 2007.

[4] Taler, J., "Theory of Transient Experimental Techniques for Surface Heat Transfer," *International Journal of Heat and Mass Transfer*, Vol. 39, No. 17, 1996, pp. 3733-3748.
doi: 10.1016/0017-9310(96)00015-4

[5] Sanderson, S. R., and Sturtevant, B., "Transient Heat Flux Measurement using a Surface Junction Thermocouple," *Review of Scientific Instruments*, Vol. 73, No. 7, 2002, pp. 2781-2787.
doi: 10.1063/1.1484255

[6] Marineau, E. C., and Hornung, H. G., "Modeling and Calibration of Fast-response Coaxial Heat Flux Gages," *47th AIAA Aerospace Sciences Meeting*, Orlando, Florida, January 5-8, 2009.

[7] Homepage of Shock Wave Laboratory, RWTH Aachen University, Germany, http://www.swl.rwth-aachen.de/en/industry-solutions/thermocouples/

[8] Li, J. P., Chen, H., Zhang, S. Z., Zhang, X. Y., and Yu, H. R., "On the Response of Coaxial Surface Thermocouples for Transient Aerodynamic Heating Measurements," *Experimental Thermal and Fluid Science*, Vol. 86, 2017, pp. 141-148.
doi: 10.1016/j.expthermflusci.2017.04.011

[9] Bendersky, D. A., "A Special Thermocouple for Measuring Transient Temperatures," *Mechanical Engineering*, Vol. 75, 1953, pp. 117–121.

[10] Alkidas, A. C., "Heat Transfer Characteristics of a Spark-Ignition Engine," *Journal of Heat Transfer*, Vol. 102, No. 2, 1980, pp. 189–193.
doi: 10.1115/1.3244258

[11] Qiao, Y. M., Chandra, S., "Boiling of Droplets on a Hot Surface in Low Gravity," *International Journal of Heat and Mass Transfer*, Vol. 39, No.7, 1996, pp. 1379–1393.
doi: 10.1016/0017-9310(95)00220-0

[12] Wang, Q., Li, J. P., Zhao, W., and Jiang, Z. L., "Influence of Thermal Sensor Installation on Measuring Accuracy at Stagnation Points," *Journal of Thermophysics and Heat Transfer*, Vol. 31, No. 2, 2017, pp. 318-323.
doi: 10.2514/1.T4971

[13] Wang, Q., Li, J. P., Zhao, W., and Jiang, Z. L., "Comparative Study on Aerodynamic Heating under Perfect and Nonequilibrium Hypersonic Flows," *Science China Physics, Mechanics & Astronomy*, Vol. 59, No. 2, 2016, pp. 624701.
doi: 10.1007/s11433-015-5708-1

[14] Peng, Z. Y., Shi, Y. L., Gong, H. M., Li, Z. H., and Luo, Y. C., "Hypersonic Aeroheating Prediction Technique and Its Trend of Development," *Acta Aeronautica et Astronautica Sinica*, Vol. 36, No. 1, 2015, pp. 325-345.
doi: 10.7527/S1000-6893.2014.0242

[15] Buttsworth, D. R., "Assessment of Effective Thermal Product of Surface Junction Thermocouples on Millisecond and Microsecond Time Scales," *Experimental Thermal and Fluid Science*, Vol. 25, 2001, pp. 409–420.
doi: 10.1016/S0894-1777(01)00093-0

[16] Jiang, Z. L., and Yu, H. R., "Theories and Technologies for Duplicating Hypersonic Flight Conditions for Ground Testing," *National Science Review*, Vol. 4, No. 3, 2017, pp. 290-296.
doi: 10.1093/nsr/nwx007

[17] Meng, B. Q., Han, G. L., Zhang, D. L., and Jiang, Z. L., "Aerodynamic Measurement of a Large Aircraft Model in Hypersonic Flow", *Chinese Physics B*, Vol. 26, No. 11, 2017, pp. 114702.
doi: 10.1088/1674-1056/26/11/114702

[18] ITS-90 table for Type E thermocouple, NIST.

[19] Schultz, D. L., and Jones, T. V., "Heat Transfer Measurements in Short Duration Hypersonic Facilities," Technical Report, AGARD-AG-165, University of Oxford, 1973.

[20] ASTM, "Manual on the Use of Thermocouples in Temperature Measurement," ASTM Special Technical Publication 470B, American Society for Testing and Materials, Philadelphia, 1981.

[21] Hoffmann, K. A., and Chiang, S. T., *Computational Fluid Dynamics*, 4th ed., Engineering Education System, Wichita, Kansas, 2000.

## Highlights

1 Different model materials result in different heat flux rates in experiments

2 Lateral heat conduction between sensor and materials exists due to their different thermal properties

3 Stainless steel (304) is suggested as model material in impulse facilities

4 A stainless steel tube is effective to improve the performance of aluminum models